

Supplementary Information

Note 1. Fluorescence Measurement

1. The photobleaching effects related to laser power

2 μl of 88 μM resorufin sodium salt (Sigma-Aldrich, Germany) was emulsified by two copies of four-chamber gravity-driven step emulsification device. We took one photo by using one laser power in each one chamber and obtained the relative fluorescent intensity by using image J. The results showed that when the laser power reached 80%, it started photobleaching.

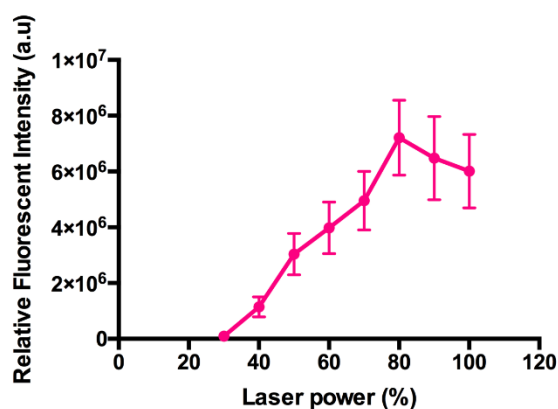


Fig. S1 The relative fluorescent intensity of resorufin versus laser power (%) of the confocal microscopy.

2. Definition of positive droplets

Images taken using confocal microscope (Nikon A1R/TiE, Japan) were loaded into Image J software and the value of the threshold was manually adjusted to convert these images to binary form. The function “Watershed” was used to separate the droplets from the background. The image analysis was performed by the function “Analyze Particles” and the results were added to “ROI Manager” and these transformed images were saved as masks. The original images were loaded into Image J again and then “Overlay” with the corresponding masks from “ROI Manager”. The grey values for all “ROI manager” were measured and analyzed in Excel. The threshold of 390000 a.u used to distinguish positive and negative droplets was determined by analysis of the image taken from the experiment with the concentration of 5×10^5 CFU/ml because in this case we could clearly see two groups of droplets in the histogram.

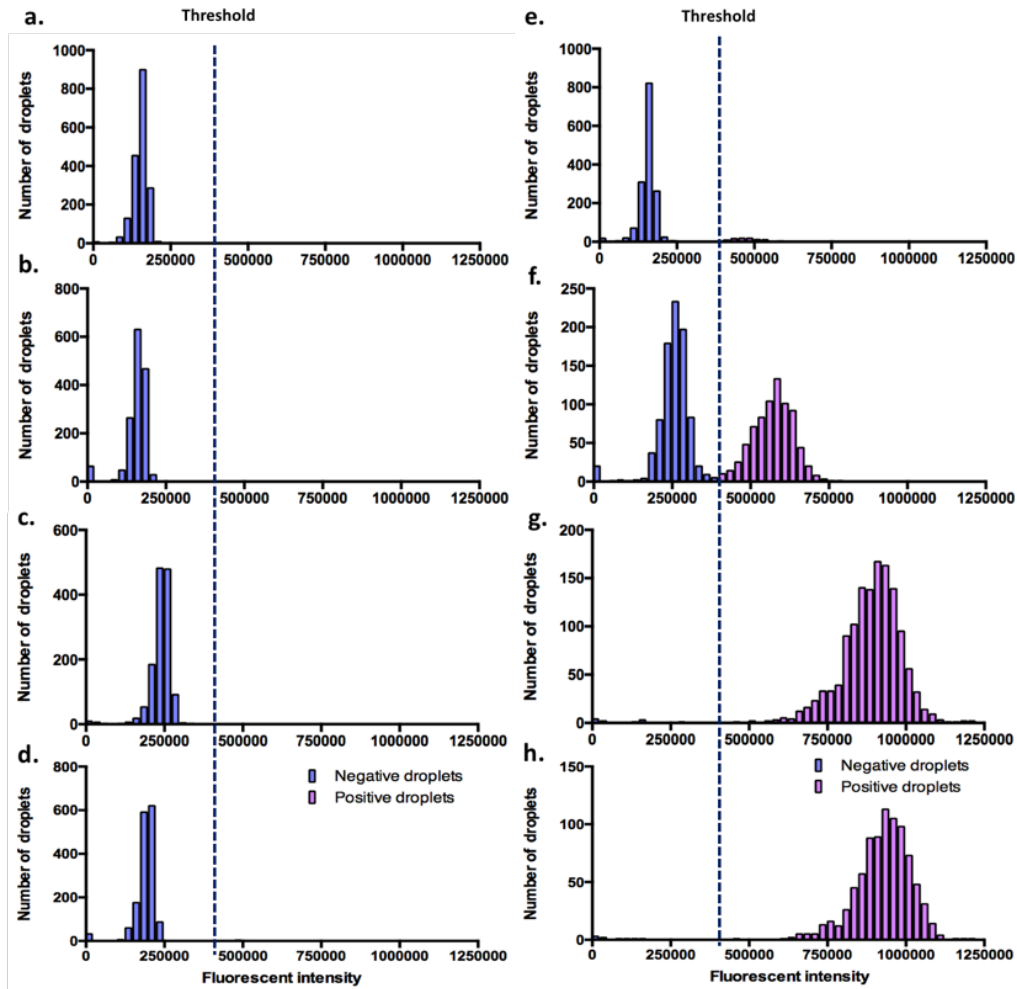
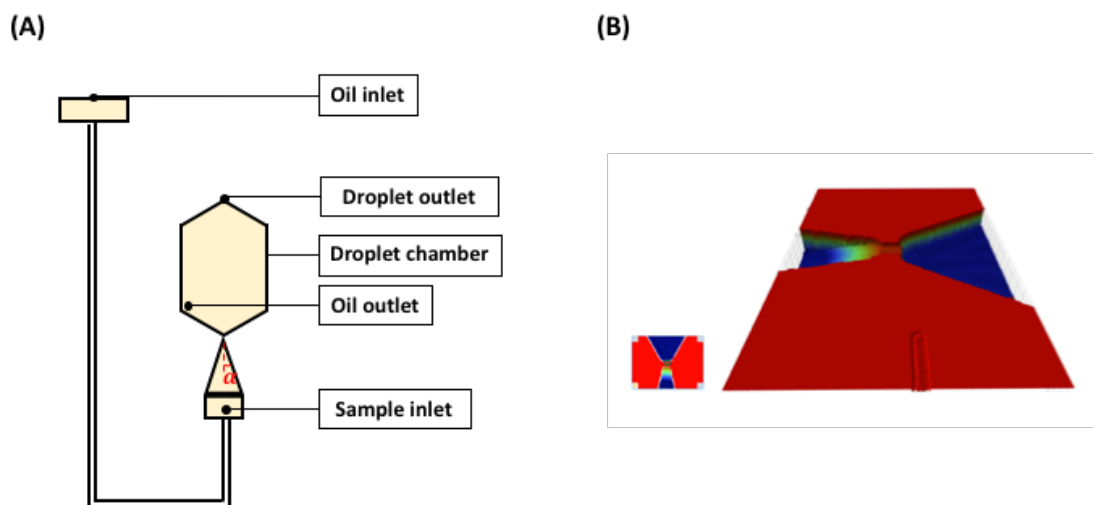


Fig. S2 Histogram of fluorescence intensity. (a) 5×10^0 CFU/ml. (b) 5×10^1 CFU/ml. (c) 5×10^2 CFU/ml. (d) 5×10^3 CFU/ml. (e) 5×10^4 CFU/ml. (f) 5×10^5 CFU/ml. (g) 5×10^6 CFU/ml. (h) 5×10^7 CFU/ml. (Blue: Negative droplets, Pink: Positive droplets)

Note 2. Three different designs with various angles of nozzle in single nozzle device.



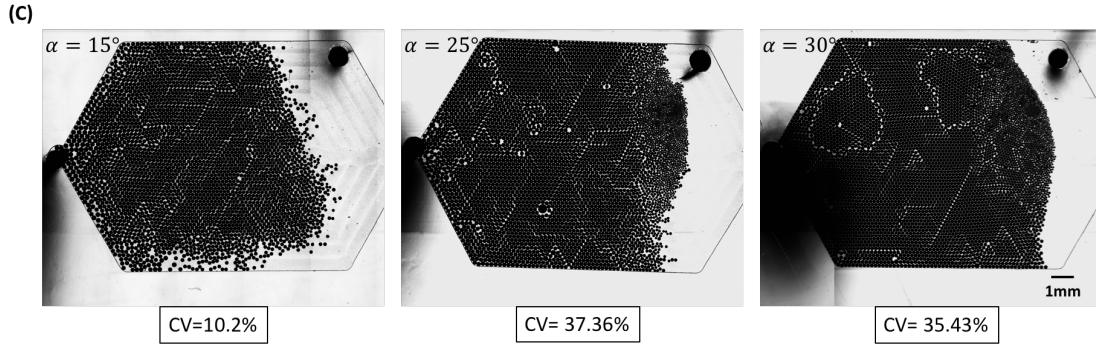


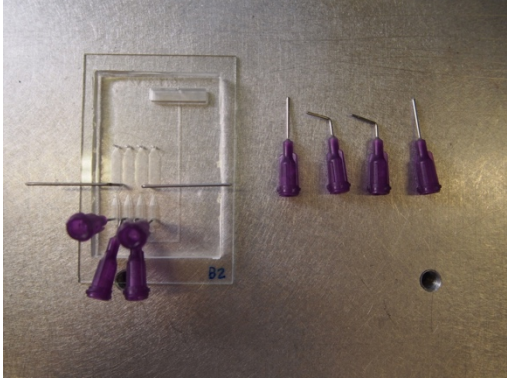
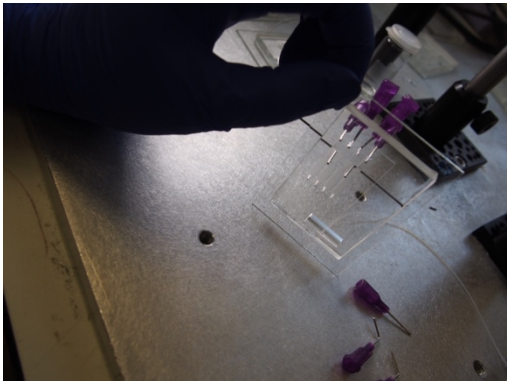
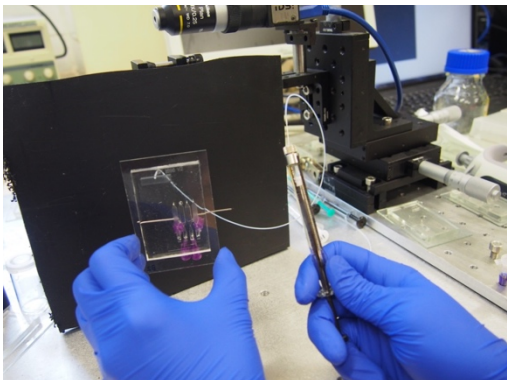
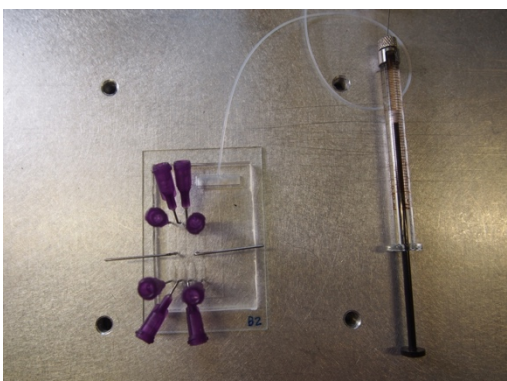
Fig. S3 The comparison of the coefficient variance of the volume of droplets generated using single nozzle devices with various different opening angles $\alpha=15^\circ$, 25° , 30° (A) The design of a single nozzle device. (B) The 3D geometry of the $\alpha=15^\circ$ device measured by Bruker ContourGT-K optical profilometer (Bruker, USA). (C) The snapshots with top views of the devices with droplets generated in devices with various opening angles $\alpha=15^\circ$, 25° , 30° , respectively The CV values presented below the snapshots correspond to the level of droplet polydispersity.

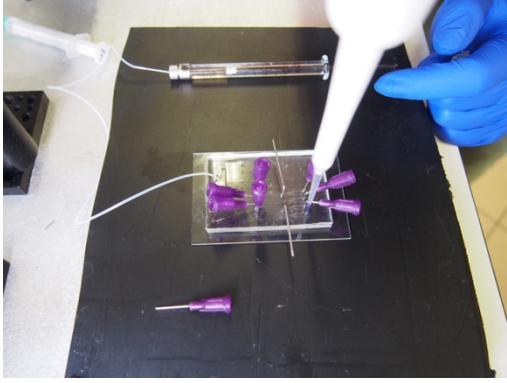
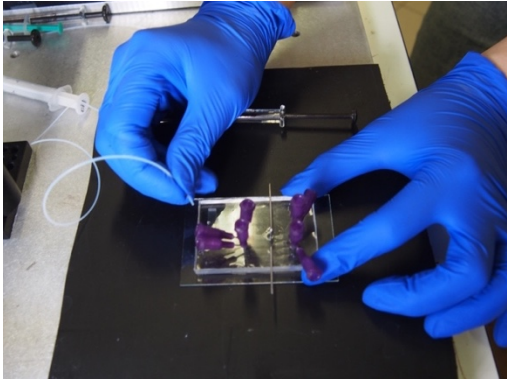
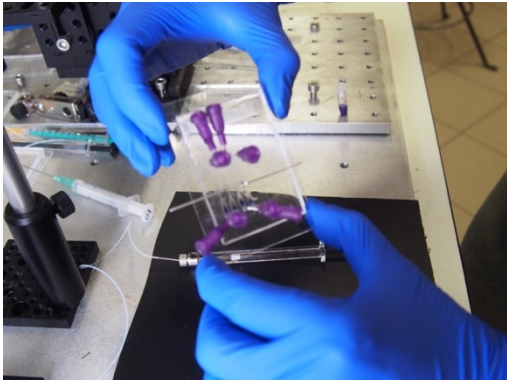

Note 3 The characterization of four-chamber gravity-driven step emulsification device

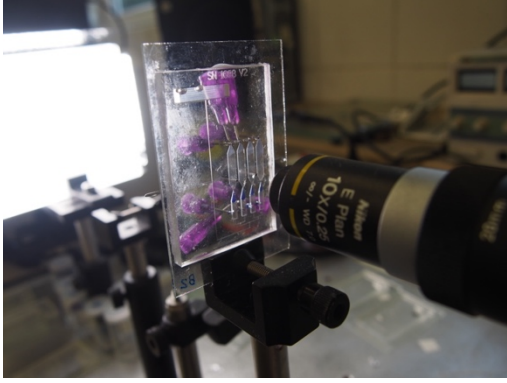
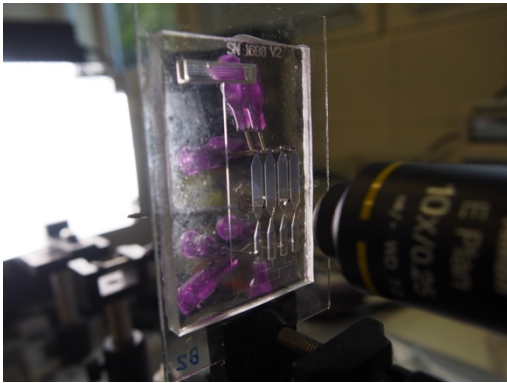
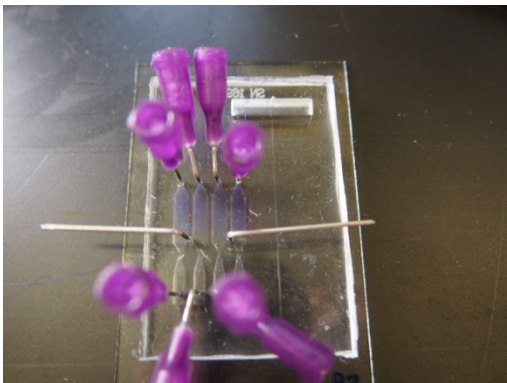
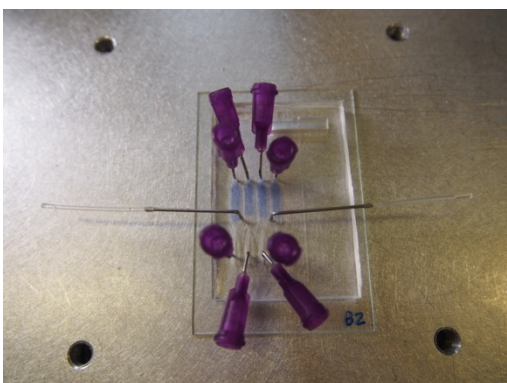
1.

Table S1. The protocol of using four-chamber gravity-driven step emulsification device

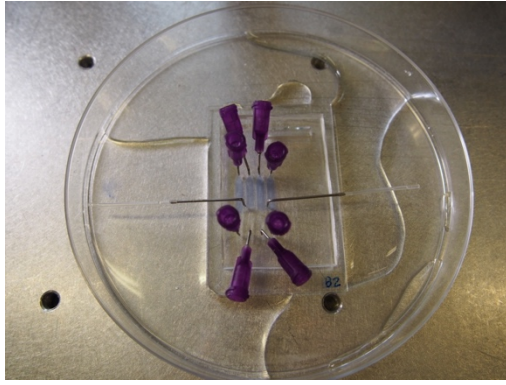
NO.	Steps	Description
1		<p>4 closed needles (To close the sample inlets)</p> <p>2 open tube (oil outlet)</p>

2	 A clear microfluidic chip is shown on a metal surface. It has several purple valves attached to its sides. A thin metal rod is positioned across the top of the chip. The number '82' is visible on the bottom right of the chip.	Close the sample inlets
3	 A person's hand is shown using a syringe to fill a port on the microfluidic chip. The chip is held in a black frame. The background shows a laboratory setting with various equipment.	Fill the oil from oil inlet. Rotate the chip by 180 degrees to fill the oil reservoir.
4	 A person wearing blue gloves is holding the microfluidic chip, which is mounted on a black frame. They are using a thin metal rod to rotate the chip. The background shows laboratory equipment.	Turn the chip back and still filling the oil until all the chambers filled with oil.
5	 The microfluidic chip is shown on a metal surface. A syringe is connected to one of the ports on the chip. The chip has purple valves and a thin metal rod across it. The number '82' is visible on the bottom right of the chip.	Close the sample outlet

6	 A person wearing blue gloves is using a white pipette to deposit a purple liquid into a clear microfluidic chip. The chip is held in a metal frame. A syringe and another pipette are visible on the black surface below.	Open the sample inlet and deposit the sample by pipetting
7	 A person wearing blue gloves is holding the microfluidic chip and using a syringe to open the oil inlet. The chip is held in a metal frame.	Open the oil inlet
8	 A person wearing blue gloves is holding the microfluidic chip and turning it to a vertical position. The chip is held in a metal frame.	Turn the chip to the vertical position
9	 A laboratory setup for droplet generation. A computer monitor displays data, and a microscope is positioned to observe the chip. A syringe and other equipment are visible on the table.	Droplet generation

10	 <p>A close-up view of a microfluidic device held in a black clamp. A microscope objective lens, labeled 'E Plan 10X/0.25', is positioned to the right, focusing on the device. The device has a transparent top layer with a grid of small chambers. Purple liquid is visible within these chambers, and small droplets are being formed at the outlets.</p>	The zoom to the device during the process of droplet generation
11	 <p>A similar view to the previous image, showing the device after droplet generation. The purple liquid is now more concentrated in the chambers, and the droplets are more distinct. The microscope objective is still visible on the right.</p>	Droplet generation completed
12	 <p>A top-down view of the device. The purple liquid is now fully contained within the chambers, and each chamber is filled with several spherical droplets. Two thin metal rods are used to hold the device steady.</p>	Droplet chambers full of droplets
13	 <p>A top-down view of the device on a metal surface. The purple liquid is now contained within the chambers, and the droplets are still visible. Two thin metal rods are used to hold the device steady. The device is now sealed with end-sealed tubes.</p>	Close the oil outlet with the end-sealed tubes

14



Pour water to the Petri dish to prevent evaporation

2. The depth of the channel measured by Bruker ContourGT-K optical profilometer (Bruker, USA)

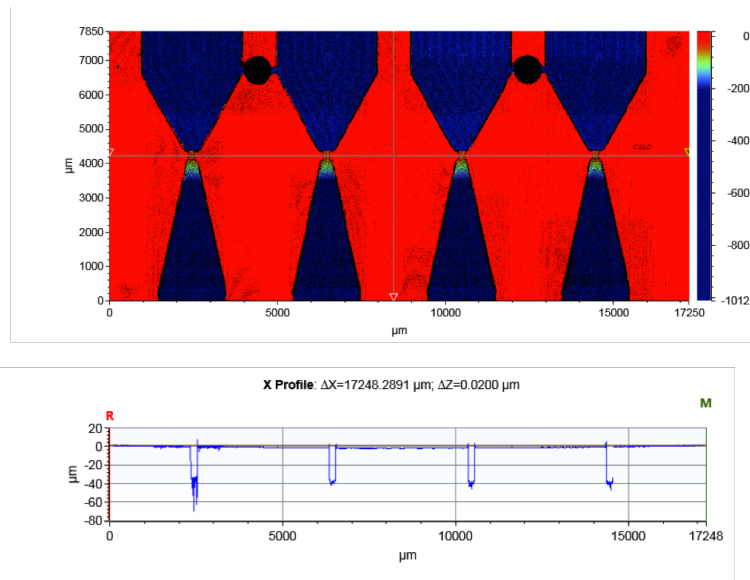


Fig. S4 The image with the profile of the device measured by Bruker ContourGT-K optical profilometer (Bruker, USA).

3. The droplet generation from four-chamber gravity-driven step emulsification device

5 μl MH broth loaded in four sample inlet that emulsified within four chambers and the volume of droplets were measured by image analysis from a recorded video.

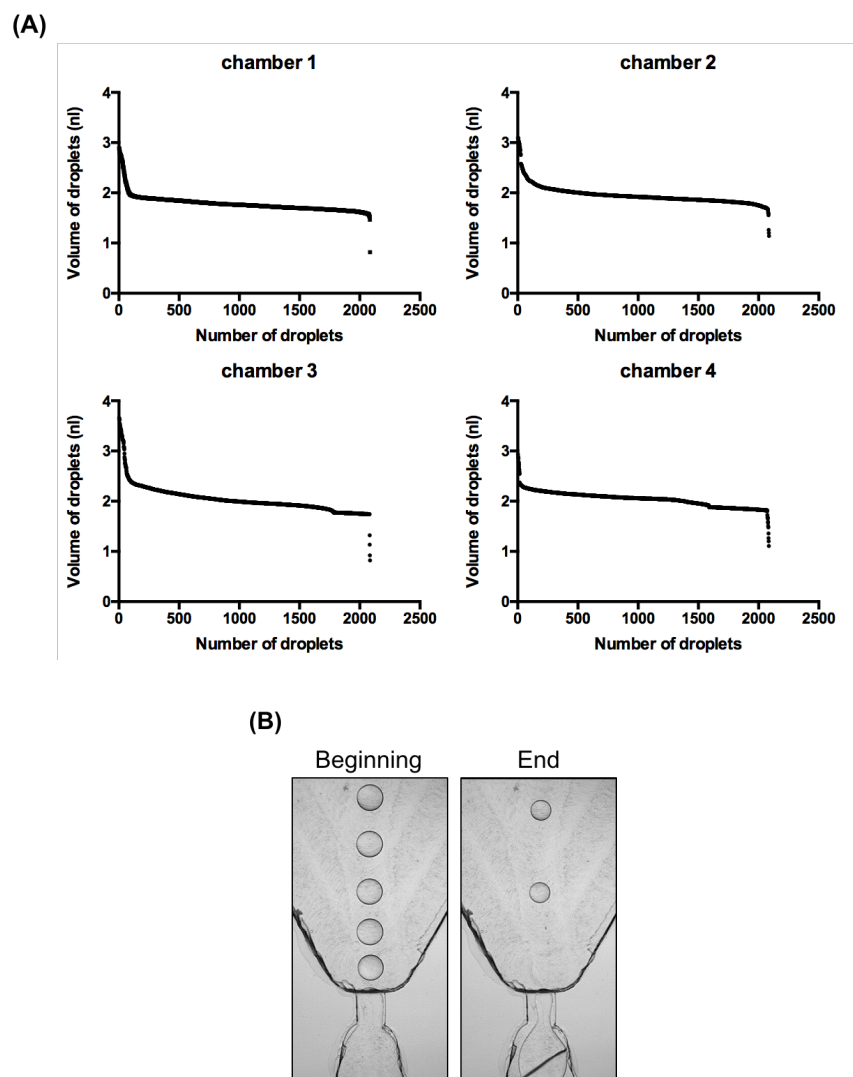
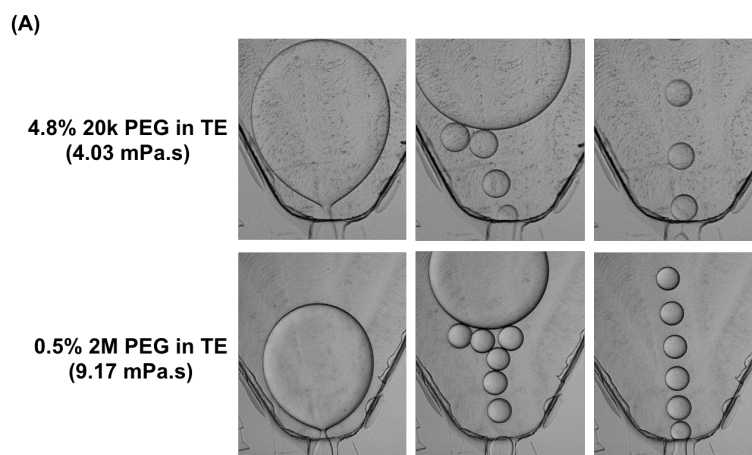


Fig. S5 The monodispersity of droplet volume in each chamber. (A) The volumes of consecutive droplets measured by image analysis. (B) The comparison of the size of the droplets in the beginning and the end of droplet generation process.

4. The “Balloon” phenomenon when the viscosity is above 4 mPa·s



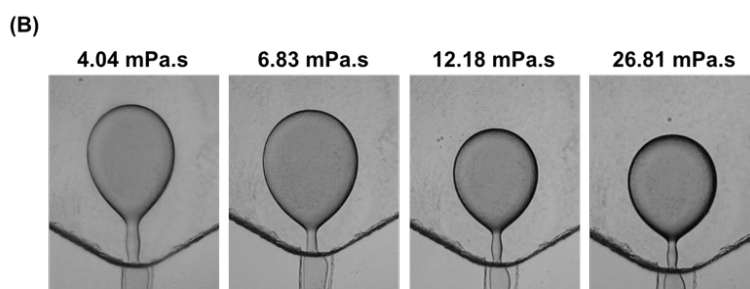


Fig. S6 Balloon phenomenon observed when the viscosity was above 4 mPa·s. (A) 4.8 wt% 20k PEG in TE buffer (4.03 mPa·s), and 0.5 wt% 2M PEG in TE buffer (9.17 mPa·s) emulsified in four-chamber device. (B) 45 wt% glycerol in water (4.04 mPa·s), 56 wt% glycerol in water (6.83 mPa·s), 65 wt% glycerol in water (12.18 mPa·s), and 75 wt% glycerol in water (26.81 mPa·s) emulsified in single chamber device.

5. Droplet instability with 1% surfactant

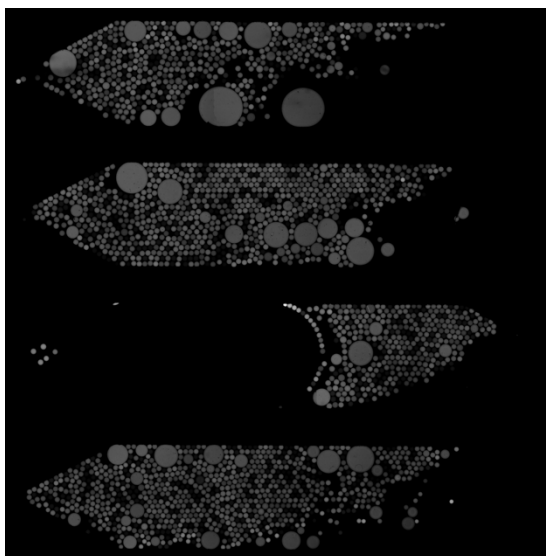


Fig. S7 Emulsion instability with external phase HFE 7500 containing 1 wt % surfactant with the oil outlets left open during incubation.

Note 4. Estimation of depletion time of oxygen

We could estimate oxygen depletion time in droplets using parameters that can be found in the literature [RSC Adv., 2015, 5, 101871]. The oxygen solubility in complex medium is ~ 0.2 mmol/L [RSC Adv., 2015, 5, 101871] and the average volume of the droplets presented here is around 2 nl. Therefore, the number of oxygen molecules in the single droplet equals 4×10^{-13} mole. In addition, the oxygen solubility in HFE 7500 used here as the continuous phase is >100 ml/L [RSC Adv., 2017, 7, 40990-40995]. In

our device, one chamber contains 12 μl HFE 7500. Thus, there will be more than 5.36×10^{-11} mole of oxygen in one droplet chamber. In one chamber, we assume we have 65% of positive droplets (ca. 1300 droplets over 2000 droplets) so each positive droplet will obtain 4.12×10^{-14} mole of oxygen from oil. Hence, each positive droplet can obtain 4.41×10^{-13} mole oxygen from oil and the medium. Therefore, it would take 6 hours for bacteria to completely consume oxygen present in droplets.

The consumption of oxygen by bacteria by time:

$$\frac{dA_0}{dt} = N(t) \cdot O_r \quad (1.1)$$

$$A_0(t) = A_0(0) - O_r \int_0^t N(t) dt \quad (1.2)$$

The growth of bacteria by time:

$$N(t) = N_0 e^{kt} \quad (1.3)$$

$$k = \frac{\ln 2}{t_d} \quad (1.4)$$

So, the remaining amount of oxygen is:

$$A_0(t) = A_0(0) - O_r \frac{N_0}{k} (e^{kt} - 1) \quad (1.5)$$

Where,

$A_0(t)$: Amount of oxygen in droplet at time t;

$A_0(0)$: initial oxygen amount in droplet;

$N(t)$: number of bacteria inside droplet at time t;

O_r : Oxygen uptake rate per single bacterium = $0.9 \sim 23.1 \text{ mol kg}_{\text{DCW}}^{-1} \text{h}^{-1}$;

N_0 : initial bacteria number;

t_d : *E. coli* doubling time = 0.5 hour

Table S2. Parameters used for calculation of oxygen depletion time

Dry cell weight (DCW)	$2.78 \times 10^{-16} \text{ kg/cell}$
Oxygen uptake rate	$0.9 \sim 23.1 \text{ mol} \cdot \text{kg}_{\text{DCW}}^{-1} \text{h}^{-1}$
Oxygen solubility in complex medium	$\sim 0.2 \text{ mmol/L}$
Oxygen solubility in HFE 7500	$> 100 \text{ ml/L}$

Note 5. Calibration curves relating OD measurements (600 nm) versus plate counting in CFU/ml

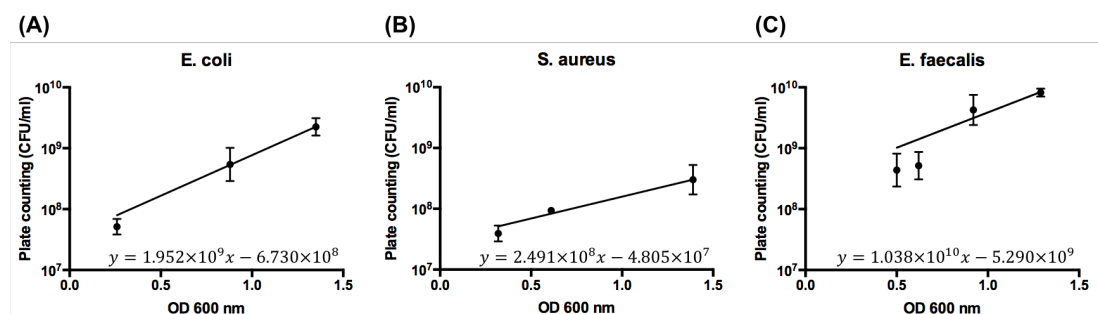


Fig. S8 Calibration curves relating OD measurements (600 nm) versus plate counting in CFU/ml for (A) *E. coli* (B) *S. aureus* (C) *E. faecalis*.

Note 6. Fraction of positive droplets as a function of bacteria concentration for *E. coli*, *S. aureus*, and *E. faecalis*

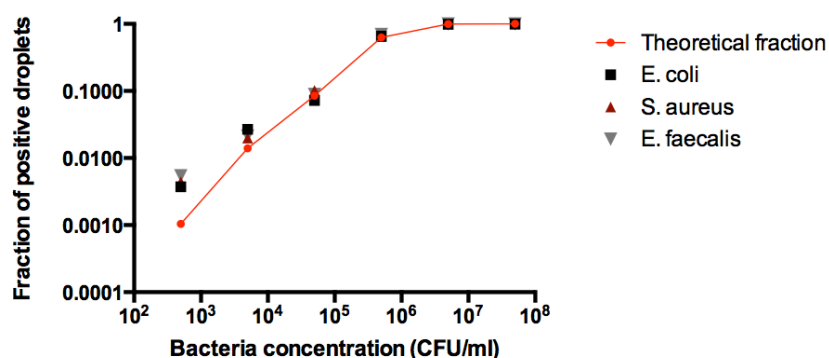


Fig. S9 Fraction of positive droplets as a function of bacteria concentration for *E. coli*, *S. aureus*, and *E. faecalis*. The red line indicates the theoretical fraction of positive droplets. (Only dilutions that are statistically relevant are shown in the plot)

Note 7. The least squares fit

The least squares fit within the logarithmic axes is done by the guidance of GraphPad website:

https://www.graphpad.com/guides/prism/6/curvefitting/index.htm?reg_fitting_lines_t_o_semilog.htm

Log-log line - Both X and Y axes are logarithmic, the correlation is

$$Y = 10^{Slope \log X + Yintercept}$$

Table S3. The statistic raw data obtained from GraphPad

		<i>E. coli</i>	<i>S. aureus</i>	<i>E. faecalis</i>
Best-fit values	YIntercept	1.902	1.384	1.787
	Slope	0.6681	0.7535	0.6981
Std. Error	YIntercept	0.2425	0.1059	0.1911
	Slope	0.03644	0.01575	0.02869
95% Confidence Intervals	YIntercept	1.131	1.047	1.179
		to	to	to
	2.674	1.721	2.395	
	Slope	0.5522	0.7034	0.6068
to		to	to	
0.7841	0.8036	0.7894		

Note 8. Broth microdilution method for determination of MIC on ampicillin against *E. coli*, cefotaxime against *S. aureus*, and ampicillin against *E. faecalis*

10^6 CFU/ml bacteria (*E. coli*, *S. aureus*, and *E. faecalis*) was mixed with 32, 16, 8, 4, 2, 1, 0.5, 0 $\mu\text{g/ml}$ of antibiotics (ampicillin and cefotaxime) and incubated at 37°C for 20 hours according to the standard broth dilution methods for MIC test from CLSI³. For visibility and imaging, we added alamar blue (Sigma-Aldrich, Germany) in each well and waiting for 2 hours for the color change. The MIC value for ampicillin against *E. coli* is 4 $\mu\text{g/ml}$, for cefotaxime against *S. aureus* is 1 $\mu\text{g/ml}$, and for ampicillin against *E. faecalis* is 0.5 $\mu\text{g/ml}$.

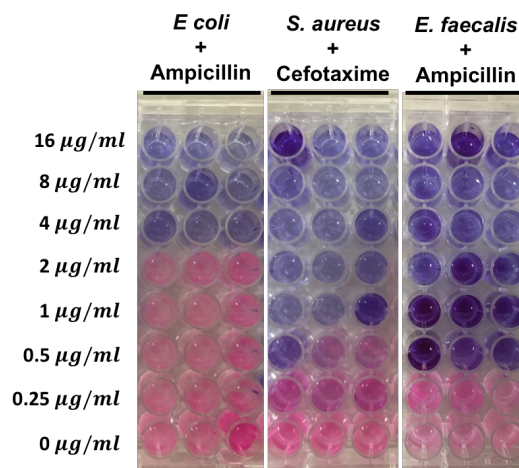
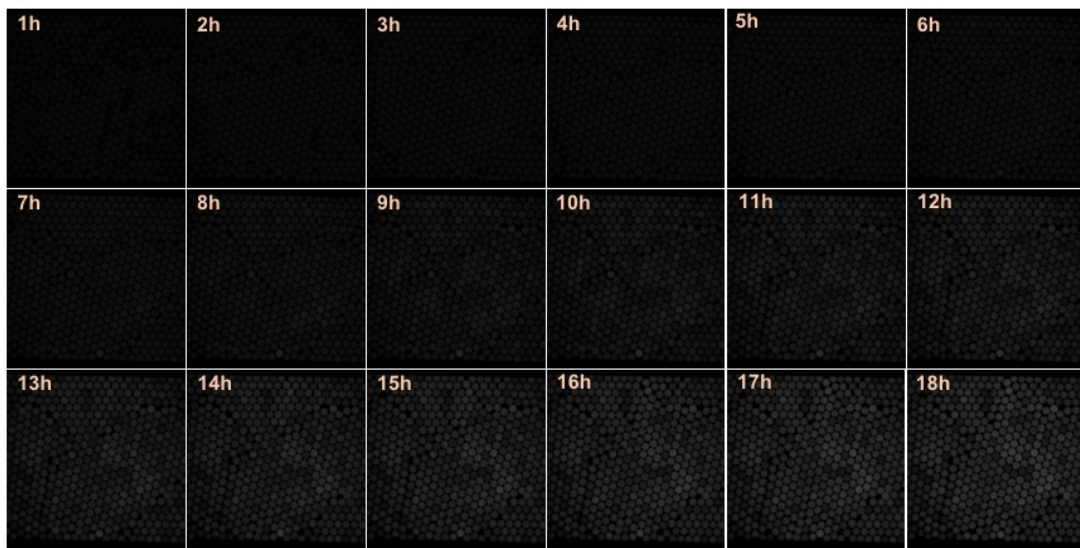


Fig. S10 Broth microdilution method for determination of MIC on ampicillin against *E. coli*, cefotaxime against *S. aureus*, and ampicillin against *E. faecalis*.

Note 9. Long-term incubation of *P. aeruginosa*.

(A)



(B)

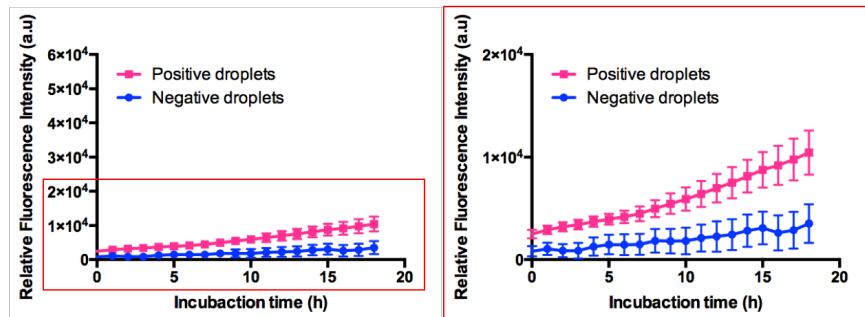


Fig. S11 Long term incubation of *P. aeruginosa* in droplets. (A) The fluorescent images taken every 1 hour by time-lapse until 18 hours. (B) The relative fluorescence intensity of positive and negative droplets versus time.

Note 10. The technical innovation of gravity-driven step emulsification device (GSED)

The flow of liquids in our device is purely powered by gravity. According to the Pascal's law the hydrostatic pressure P at the depth Δh below a free liquid surface reads

$$P = \rho g \Delta h,$$

where ρ is the liquid density, g is the gravitational acceleration; in our case, Δh is the height difference between the oil inlet and oil outlet. Droplets are generated via Laplace-pressure driven narrowing of a neck of the droplet phase (so called step emulsification) forming at the inlet chamber to the droplet chamber when the chip is placed align with gravitational field. While in the literature, the gravity-driven systems used two reservoirs/containers placed in different height to make Δh to trigger the flow and their monodispersity of droplet are vulnerable by the flow rate which is related to Δh (Table S4).

Table S4. Comparison of GSED and previous gravity-driven droplet generation device

	GSED	Zhang et al. [15]	Van Steijn et al. [16]	Tjhung et al. [17]
Droplet generation method	Step emulsification	T-junction	T-junction	Flow-focusing
Set-up of the system	All modules integrated in a single device (e.g. oil reservoir, sample chambers, droplet generators...etc.)	A turntable for hanging and adjusting the height difference of reservoirs, a vertical plastic board, several disposable infusions sets, rings, Nylon lines and droplet generators (microfluidic chips)	Two containers with continuous phase and dispersed phase connected to the droplet generator by capillaries	Two syringes filled with aqueous media and perfluorinated oil placed at different heights and a droplet generator (microfluidic chip)
Droplet generator	Optimized nozzle for passive production of monodisperse droplets	A simple T-junction	A T-junction with a bypass channel	A simple flow focusing junction
Droplet size	Fixed size by the designed height difference	Tunable size by adjusting the turntable for the height	Fixed size by fixed-volume of droplet generator	Tunable size by the height difference of two syringes

between oil reservoir and oil outlet	difference between two reservoirs
--------------------------------------	-----------------------------------

Table S5. Comparison of GSED and DropChop (Lab Chip, 2017, 17, 1323)

	GSED	DropChop
Power source	Gravity (hydrostatic pressure)	Very expensive (3500 euros net) Cetoni neMesys syringe pump
The design of emulsifier	A large sample container that is sloped in two axes.	A sloped straight channel with a sample inlet channel of 400×400 μm cross-section
Emulsify larger sample volume	Yes. Sample chamber is integrated in the emulsifier	No. The design would require 12.5 cm long channel for emulsification. Such extremely long droplet would wet the channel and/or break into several smaller droplets

Note 11. Digital droplet AST could reduce the MIC measurement errors introduced by the inoculum effect and errors in establishing the desired inoculum density

The inoculum effect generally occurs when the β -lactamase producing bacteria are exposed to β -lactam antibiotics [1]. It would manifest even within the CLSI-allowable inoculum range and serve as a source of error and inconsistency in AST determinations [2]. Here, we chose β -lactam antibiotics (ampicillin and cefazolin) against *S. aureus* ATCC 29213 which is a weak β -lactamase positive strain and β -lactam antibiotics (cefotaxime) against *E. coli* DH5 α TEM-20 which is an extended-spectrum β -lactamase producing strain to examine the inoculum effect. We assessed the MIC by broth microdilution, VITEK[®]2 system, and gravity-driven step emulsification device (GSED) and presented the results of tests in **Table S6**. The number of bacteria (5×10^5

CFU/ml) used for standard MIC in broth microdilution and GSED were counted by digital droplet CFU as we mentioned in **Fig. 5**. However, we did not know the cell density in the final inoculum for AST in VITEK[®]2 because the suggested inoculum of 0.5-0.63 McFarland if further dilution on the card through its automatic transport system. The fold of this dilution on a card is not revealed in the user manual. In addition, the McFarland suspensions of bacteria with different sizes, shapes, and clustering characteristic may yield CFU counts that differ by several fold [3]. This might be the main reason that we got different and higher value of MIC in VITEK[®]2 for ampicillin against *S. aureus* ATCC 29213 and cefazolin against *S. aureus* ATCC 29213. Another disadvantage of VITEK[®]2 is that the AST card has small number of chambers and performs truncated dilution series for a certain antibiotic which results in an incomplete MIC that shows the MIC value in a range (e.g. the MIC of cefazolin against *S. aureus* ATCC 29213 is ≤ 4).

Interestingly, we found out that in the group of tests with cefotaxime used against *E. coli* DH5 α TEM-20, the MIC value in broth microdilution method is 6.6-fold higher than VITEK[®]2 and 12.5-fold higher than GSED. We suspected that the larger absolute population size of *E. coli* DH5 α TEM-20, the more enzymes are produced and thus the higher the change in antimicrobial efficacy when there is a huge inoculum effect. In our experiment, we used 150 μ l of inoculum per well in broth microdilution method, and 2 nl inoculum per droplet in GSED. For the inoculum density of 5×10^5 CFU/ml, there will be 75000 CFU per well and 1 CFU per droplet. Moreover, the volume of the VITEK[®]2 Card chamber is approximately 18 μ l, in the case of inoculum density of 5×10^5 CFU/ml, there will be 9000 CFU per chamber. Therefore, the antibiotic will degrade very fast in broth microdilution method because of the increasing inoculum volume even though the inoculum density is the same as other methods.

We further examined the MIC value within the allowed range of starting inoculum density that CLSI ($2-8 \times 10^5$ CFU/ml) and EUCAST ($3-7 \times 10^5$ CFU/ml) recommend and found dramatic inoculum effect on MIC determination within this narrow range of inoculum densities in the group of cefotaxime against *E. coli* DH5 α TEM-20 (**Table S7**). Meanwhile, the digital droplet AST assay performed in GSED are more robust against experimental errors (**Fig. S12**) because using diluted starting inoculum, only single bacterium is encapsulated in a 2 nl droplet, which corresponds to the density of 5×10^5 CFU/ml. Further dilution of the inoculum will decrease the number of positive

droplets containing single bacterium but will not change the final density in each of positive droplets which will be equal exactly 5×10^5 CFU/ml.

Overall, the gravity-driven step emulsification device provides a standalone platform with, lower consumption of consumables and samples and higher precision of assessing MIC values than commercial automated AST systems. In addition, the nature of setting a standard inoculum density in droplets makes it possible to prevent the inoculum effects in contrast to the reference MIC method (broth microdilution) and commercial susceptibility testing panels (VITEK[®]2).

Table S6. Comparison of minimum inhibitory concentrations (MICs) of β -lactam antibiotics against β -lactamase positive bacteria assessed by broth microdilution, VITEK[®]2 and gravity-driven step emulsification device (GSED)

Antibiotic/strain	MIC ($\mu\text{g/ml}$)		
	Broth microdilution	VITEK [®] 2	GSED
Ampicillin/ <i>S. aureus</i> ATCC29213	0.125	0.5	0.125
Cefazolin/ <i>S. aureus</i> ATCC29213	0.5	≤ 4	0.5
Cefotaxime/ <i>E. coli</i> DH5α TEM-20	6.6	1	0.53

Table S7. The MIC value of β -lactam antibiotics against β -lactamase producing bacteria strains within the allowed range of starting inoculum density that CLSI and EUCAST recommend for broth microdilution method

Inoculum density (CFU/ml)	MIC ($\mu\text{g/ml}$)		
	Ampicillin/ <i>S. aureus</i> ATCC29213	Cefazolin/ <i>S. aureus</i> ATCC29213	Cefotaxime/ <i>E. coli</i> DH5 α TEM-20
2×10^5	0.125	0.5	3.4
3×10^5	0.125	0.5	4.2
4×10^5	0.125	0.5	5.3

5×10^5	0.125	0.5	6.6
6×10^5	0.125	0.5	6.6
7×10^5	0.125	0.5	9.9
8×10^5	0.125	0.5	9.9

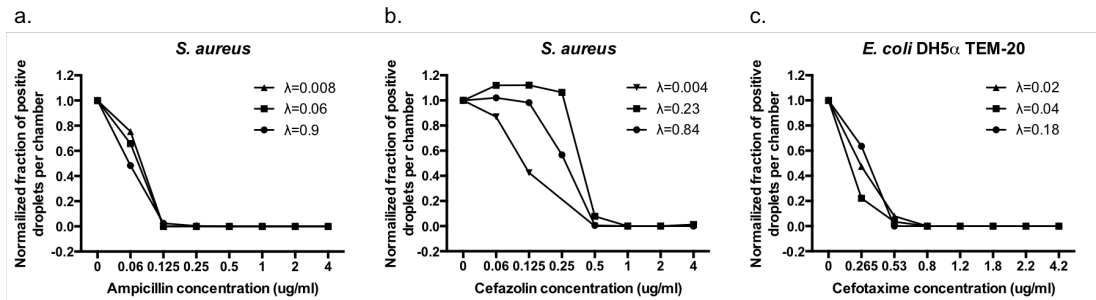


Fig. S12 Digital droplet AST are more robust against experimental errors in the initial inoculum density. **a.** ampicillin against *S. aureus* ATCC 29213. **b.** cefazolin against *S. aureus* ATCC 29213. **c.** cefotaxime against *E. coli* DH5 α . λ =average number of bacteria per 2nl droplet.

Reference

- [1] I. Brook, Clin. Infect. Dis., 1989, 11(3), 361–368.
- [2] K. P. Smith, and J. E. Kirby, Antimicrob. Agents. Chemother., 2018, 62 (8) e00433-18.
- [3] T. Brennan-Krohn, K. P. Smith, and J. E. Kirby, J. Clin. Microbiol., 2017, 55(8), 2304–2308.